Nanoscale

PAPER

View Article Online
View Journal | View Issue

Cite this: *Nanoscale*, 2021, **13**, 12910

Detecting bound polymer layers in attractive polymer–nanoparticle hybrids

Hamed Emamy, [a] Francis W. Starr[b] and Sanat K. Kumar *[a]

Received 15th April 2021,
Accepted 15th June 2021

DOI: 10.1039/d1nr02395k

rsc.li/nanoscale

When polymer–nanoparticle (NP) attractions are sufficiently strong, a bound polymer layer with a distinct dynamic signature spontaneously forms at the NP interface. A similar phenomenon occurs near a fixed attractive substrate for thin polymer films. While our previous simulations fixed the NPs to examine the dilute limit, here, we allow the NP to move. Our goal is to investigate how NP mobility affects the signature of the bound layer. For small NPs that are relatively mobile, the bound layer is slaved to the motion of the NP, and the signature of the bound layer relaxation in the intermediate scattering function essentially disappears. The slow relaxation of the bound layer can be recovered when the scattering function is measured in the NP reference frame, but this process would be challenging to implement in experimental systems with multiple NPs. Instead, we use the counterintuitive result that the NP mass affects its mobility in the nanoscale limit, along with the more expected result that the bound layer increases the effective NP mass, to suggest that the signature of the bound polymer manifests as a change in NP diffusivity. These findings allow us to rationalize and quantitatively understand the results of recent experiments focused on measuring NP diffusivity with either physically adsorbed or chemically end-grafted chains.

1. Introduction

The addition of nanoparticles (NPs) to polymers has been a topic of considerable interest because the resulting materials can have significantly improved properties (*e.g.* mechanical, optical or electrical).[1–10] The large surface-to-volume ratio of NPs implies that a significant fraction of polymer chains are interfacial, especially when we consider high NP loadings. This interfacial layer can play an important role in the resulting property modifications of the composite. In particular, we focus on how the motion and diffusion of NPs are affected by the structure and dynamics of the interfacial layer. This topic is of particular importance because the flow-related properties of these hybrid materials are of considerable interest in the context of material processing.

The spatial dispersion of NPs within the polymer matrix is another factor critical for determining property modifications.[11–13] Attractive polymer–NP interactions typically result in a thermodynamically favorable uniformly dispersed NP state.[14,15] When polymer–NP attractions exceed those between polymer segments, a "bound" layer of polymers may form near the NP interface; this bound layer has a relaxation time that can be orders of magnitude slower than that of the surrounding polymer matrix.[16–22] In previous studies,[16,21,23,24] we examined the effect of the polymer–NP interaction strength on chain (and segmental) dynamics, especially in the bound layer. In these initial studies, we limited ourselves to an idealized case of a fixed NP at low enough concentrations to understand interfacial effects without the complications of interactions among NPs. Here we remove the constraint of a fixed NP, to study the effect of NP motion on the dynamics of the bound layer, and how the presence of the bound layer affects the translational and rotational motion of NPs. We find that NP motion effectively masks the distinct signature of the bound layer relaxation in the intermediate-scattering function that occurs for a fixed NP, with this effect particularly manifesting when the NP can reorient or translate on a time scale less than that of the bound layer relaxation. In the case we study, the primary reason for the disappearance of the bound layer signal in the scattering function is the rotational motion of the NP; translational motion is considerably slower. The signature of this bound layer relaxation, which we had reported in our previous work, can be recovered if the scattering function is calculated in a frame of reference moving with the particle. Experimentally, such a change of frame is a challenging task, especially with multiple NPs, and hence we need other methods to indirectly detect such a bound component. To this end, we show that the NP diffusion coefficients are particularly sensitive to the amount of the bound polymer. Specifically, by

[a]*Department of Chemical Engineering, Columbia University, New York, New York 10027, USA. E-mail: sk2794@columbia.edu*
[b]*Department of Physics, Wesleyan University, Middletown, CT 06459, USA*

comparing the case of NPs with and without a bound polymer, we find that the presence of the bound layer slows the NP diffusion. More interestingly, we demonstrate that, if we redefine the effective size of the NP to account for the volume (or mass) of the chains bound to a NP, then the diffusion coefficient of the NP matches that of a larger NP with no bound polymer. This observation provides a simple means of experimentally measuring and characterizing the bound polymer layer in these composites.

2. Simulation model and methods

Our simulation model follows the simulation parameters and protocols we have used in earlier studies.[14,16,25] Polymer chains are described *via* the Kremer–Grest model[26] with a chain length of 20, where each monomer has a diameter σ; all distances are described in units of σ. Non-bonded monomers interact *via* a truncated and shifted Lennard–Jones (LJ) potential with a cutoff distance of $r_c = 2.5$ in order to include the effect of attractions between two chain monomers; all energies are reported in units of the LJ energy parameter ε. Bonded monomers are linked by a finitely-extensible nonlinear elastic (FENE) potential, with "stiffness" $k_0 = 30\varepsilon/\sigma^2$ and maximum extension $R_0 = 1.5$. As discussed below we use a relatively small nanoparticle to ensure that it readily moves within the polymer matrix. We also simulate systems with the NP fixed at the origin. Like our earlier work that examined the factors controlling the clustering of mobile NPs,[14] each NP is composed of 13 beads (identical to the monomers of polymer chains). These 13 beads are bonded to form an icosahedron of edge length 2.1 (one monomer at each of the 12 vertices of the icosahedron, plus a single bead at the center of the icosahedron). Because of its small size and the symmetry of the icosahedron, we do not expect our results to be significantly different from those with spherically symmetric NPs with a rough surface; by extension our results may not be valid for anisotropic NPs. Further details of the NP model can be found in ref. 14. The NP size can be converted to an approximate diameter through $d = \frac{\sqrt{3}}{6}(3+\sqrt{5})a$, where a is the vertex-to-vertex distance, and d is the diameter of an inscribed sphere that touches the faces of the icosahedron; the resulting diameter is $d = 3.3$. There is an attractive LJ interaction between beads forming the NP and monomers of the polymer chains; this interaction is also truncated at 2.5. We use a variable polymer–NP interaction strength ε_{p-NP} in a series of simulations. We consider multiple volume fractions (ϕ = 0.005, 0.011, and 0.016) by varying the box size (and hence the number of chains) while keeping a single NP in the system. All units are reported in reduced units, where m is the unit of mass and ε/k_B is the unit of temperature, where k_B is the Boltzmann constant and the unit of time is $\sigma\sqrt{m/\varepsilon}$. Considering a simple polymer such as polystyrene with a glass transition temperature $T_g \approx 100$ °C, these units can be approximately converted to real units by choosing $\sigma \approx 2$ nm, $\varepsilon \approx 10$ kJ mol^{-1}, $m \approx 0.5$ kg mol^{-1}, and one time unit ≈15 ps. The chain length simulated can be mapped to molecular weight ≈10 kg mol^{-1}, below the entanglement molecular weight.

The simulations are performed using the LAMMPS[27] simulation package. We first perform a simulation at relatively high temperature ($T = 1.0$) and $P = 0.1$. We generate equilibrium configurations at lower T by reducing the temperature to the desired T (still at pressure $P = 0.1$) and allowing the system to relax long enough that the potential energy and volume reach a steady state; typically, this time is 10 to 100 times the relaxation time we report in the Results section. Using the average volume of the system from these NPT simulations, we then perform data collection simulations in the NVT ensemble along the established isobaric path ($P = 0.1$) at temperatures $0.45 < T < 0.5$. These fixed box size simulations avoid complications in the analysis introduced by a fluctuating box size at fixed pressure.

3. Results

To begin, we examine how the motion of the NP in the polymer matrix affects the dynamical signature of the bound interfacial layer, as compared to the case when NPs are fixed at the origin. We use the self-intermediate scattering function to quantify the dynamics of the polymer, namely

$$F_{self}(q,t) = \frac{1}{N}\left\langle \sum_{j=0}^{N} e^{i\mathbf{q}\cdot(\mathbf{r}_j(t)-\mathbf{r}_j(0))} \right\rangle \quad (1)$$

where $\mathbf{r}_j(t)$ is the location of monomer j at time t and q is the scattering wave vector. We evaluate $F_{self}(q, t)$ at $q_0 = 7.1$, which corresponds to the first peak of the static structure factor of polymer segments. In our previous work with a fixed NP,[16] we found that $F_{self}(q, t)$ shows three distinct relaxation processes when polymer–NP interactions become more favorable than polymer–polymer interactions. These three relaxations can be quantitatively described by:

$$F_{self}(q,t) = (1-A)e^{-(t/\tau_s)^{3/2}} + (A-A_b)e^{-(t/\tau_\alpha)^{\beta}} + A_b e^{-(t/\tau_b)^{\beta_b}}. \quad (2)$$

The fastest relaxation time τ_s describes the vibrational motion of monomers; the intermediate relaxation time τ_α corresponds to the primary or α relaxation process, associated with the relaxation of the polymer segments in the matrix; finally, the slowest relaxation time τ_b is related to the bound interfacial layer. A and A_b are the amplitudes of vibrational relaxation and bound layer relaxation signals, respectively. While the signature for the bound polymer is clear in Fig. 1, the effect of the bound polymer is less pronounced for the small NP as relative to a larger NP; this aspect has been discussed in ref. 21. In marked contrast, when the NP is free to rotate and translate, the behavior of $F_{self}(q, t)$ is qualitatively different: the slowest bound interfacial layer relaxation appears to disappear.

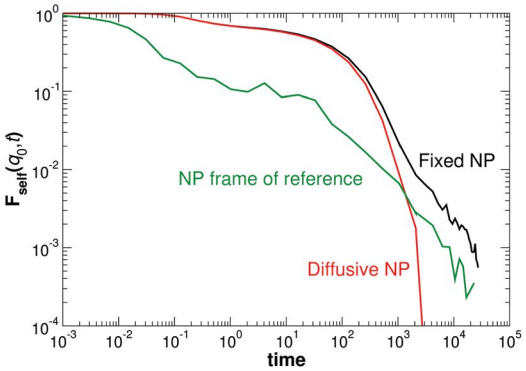

Fig. 1 The intermediate scattering function $F_{self}(q_0t)$ of monomers for a fixed NP (black line) and a diffusive NP (red line) at T = 0.46, ϕ = 0.011 and ε = 2.0. There is a third distinct relaxation process in the system with the fixed NP that is apparently missing from the system with the diffusive NP. The scattering function in the NP frame of reference (green line) shows the presence of the long-time relaxation, presumably corresponding to the bound layer around the NP.

Clearly, NP motion plays an important role, but these data alone do not clarify if the motion of the NP prevents the formation of the bound layer around it. Alternatively, a bound layer may exist, but the motion of the NP may lead to relaxation that masks its distinct signal in $F_{self}(q_0t)$. To distinguish between these two possible scenarios, we calculate the $F_{self}(q_0t)$ in the NP frame of reference, where the frame of reference translates and rotates with the NP. Fig. 1a shows that in this frame, a slow relaxation re-emerges. Thus, a bound layer (a layer with very slow dynamics relative to the NP) does form around the NP, but the NP motion masks this signal in the "lab" reference frame.

There is no obvious way to switch to the NP reference frame experimentally, especially in a system with multiple NPs, and so the measurement of the bound signal *via* the scattering function would be challenging, if not impossible.

The disappearance of the bound layer signal is a reflection of the fact that the NP mobility (through either translation or rotation) is faster than the relaxation rate of the bound layer around the NP. Thus, if one could reduce the mobility of the NP relative to the bound polymer, the signal for the bound layer might again be apparent in the lab frame. Accordingly, we consider changing the NP properties to reduce its mobility, and in doing so, we uncover an unexpected alternative approach to identify the presence of the bound layer. While the Stokes–Einstein relation implies that the diffusion of a particle is independent of mass, this idea is likely valid only when the relaxation of the medium is much faster than the relaxation of the Brownian particle. Instead, for a small NP (where the NP radius R_{NP} is comparable or smaller than the chain radius of gyration, R_g), the dynamics of the NP will be on the same time scale as that of the polymer chains. Thus, the diffusion of the NP can be sensitive to the mass of the NPs, as has been found previously.[28,29]

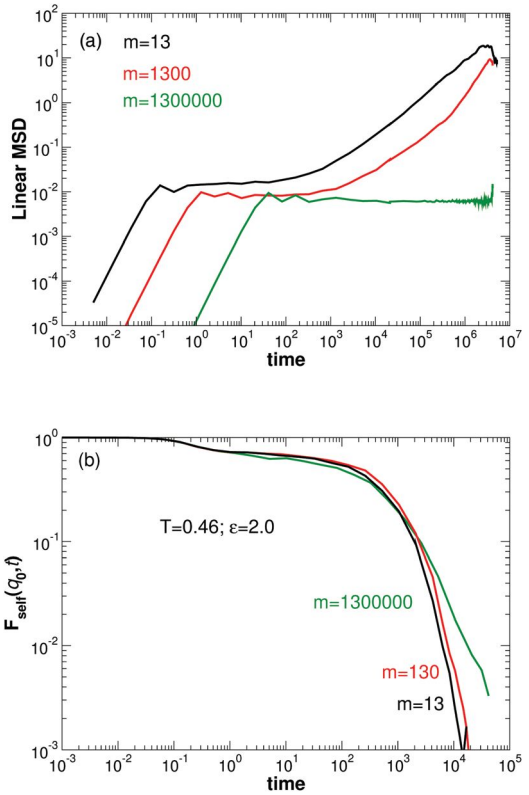

Fig. 2 (a) Altering the NP mobility by changing its mass. The NP mean-squared displacement $\langle r^2 \rangle$ is reduced by increasing the mass of its constituent sites. (b) Scattering function for systems with different NP masses. The bound relaxation time is clear for the heaviest NP. The bound layer relaxation, with a time constant of τ_b, is partially recovered for the heavier mass NP.

Accordingly, as a first step toward identifying a bound layer signal, we consider how the mass of the NP affects its mobility and the associated scattering data for the polymer. Fig. 2(a) shows the NP mass dependence of the translational mean-squared displacement (MSD)

$$\mathrm{MSD}_{\mathrm{trans}}(t) = \left\langle (\vec{r}(t) - \vec{r}(0))^2 \right\rangle, \quad (3)$$

where $\vec{r}(t)$ is the position of the center of the NP at time t. Clearly, increasing the NP mass decreases its translational mobility. We evaluate the intermediate-scattering function for different NP masses in Fig. 2(b) and find that there is a restoration of the bound layer signal for a large NP mass, supporting our assertion that the bound signal can be experimentally accessible if the NP mobility is small compared to the polymer matrix.

Next, we distinguish the contributions from the rotational and translational motion of the NP to the "loss" of the bound layer signal. We have already introduced the translational MSD, and the rotational MSD is defined by,

$$\mathrm{MSD}_{\mathrm{rot}}(t) = \left\langle \left(\vec{\phi}(t) - \vec{\phi}(0) \right)^2 \right\rangle, \quad (4)$$

where

$$\vec{\phi}(t) = \int_0^{t'} \Delta\vec{\phi}(t')\mathrm{d}t'. \quad (5)$$

$\Delta\vec{\phi}(t)$ is defined as the cross product of the position of the vertices of the NP (which is an icosahedron) relative to the center of the icosahedron $\Delta\vec{\phi}(t) = \vec{u}(t+\Delta t) \times \vec{u}(t)$. The rotational MSD also defines the squared arc-length displacement of the rotation

$$\langle s^2(t)\rangle = \left(\frac{d}{2}\right)^2 \mathrm{MSD}_{\mathrm{rot}}(t), \quad (6)$$

where d is the diameter of the NP. The arc length $\langle s^2\rangle$ is convenient to compare against the translational MSD, since it has the same units and describes the motion of the NP surface. Fig. 3 shows that $\langle s^2\rangle$ is larger than $\mathrm{MSD}_{\mathrm{trans}}$, indicating that the rotational diffusion plays a more significant role in the diminishing of the bound layer relaxation time signal in the $F_{\mathrm{self}}(q,\ t)$. We examine this assumption by calculating the $F_{\mathrm{self}}(q_0 t)$ where we just remove the translational motion of the NP and keep its rotational motion. Fig. 3(b) shows that the bound layer relaxation is suppressed when rotation is included but the translational motion of the NP is removed. This result confirms that the rotational motion of the NP is the primary contribution to relaxation that masks a bound polymer signal in $F_{\mathrm{self}}(q_0 t)$.

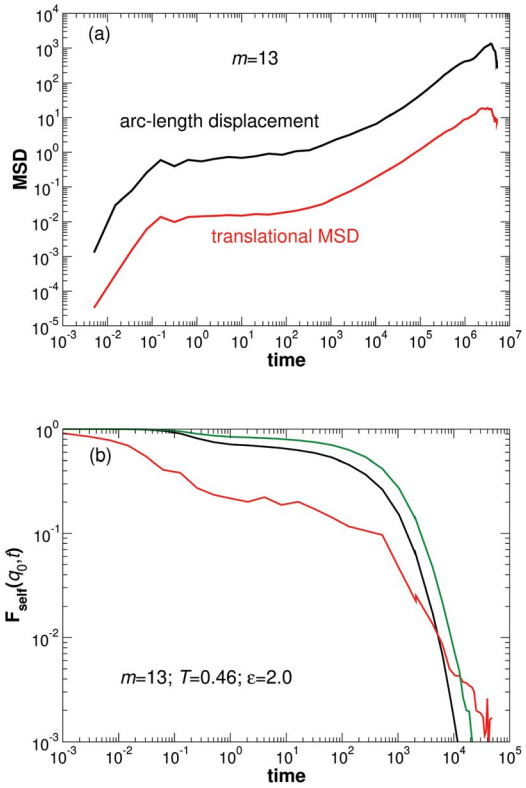

Fig. 3 (a) The translational MSD and rotational arc-length displacement (s) of the NP. The rotational motion has a larger displacement compared to translational motion. (b) Scattering function $F_{\mathrm{self}}(q_0 t)$ of monomers for moving the NP (black), in the frame of reference of the NP that rotates with the NP (red) and in the frame of reference not rotating with the NP (green). The absence of the bound layer signal in the green curve further confirms the importance of the rotational motion.

The dependence of NP mobility on mass gives rise to a possible alternative approach to quantify the effect of the bound layer on measurable properties. However, before we proceed it is important to stress a few points. It is well known that the mass of the particles affects viscosity; since our intent is to consider the tracer diffusion coefficient of a NP of variable mass in a sea of solvents (with fixed mass), it is reasonable to assume that the viscosity of the solution is not variable. Of course, this will not be true for finite NP concentrations, and hence we proceed with this caveat in mind. Since the bound layer is closely associated with the NP, one can consider that an increase in its effective mass leads to an apparent increase in the NP size, thus rationalizing the reduction in its mobility. Said differently, the mass of the polymer in the bound layer may manifest itself through a slowdown of the NP diffusion in the polymer matrix; if true, this could be readily accessible in experiments and allow us to quantify this hard-to-measure quantity. To understand the role of the NP mass increase in the diffusion coefficient of NPs we studied systems with ($\varepsilon_{\mathrm{p-np}}$ = 2.0; T = 0.5) and without ($\varepsilon_{\mathrm{p-np}}$ = 1; T = 0.5) the bound layer. For PNCs without the bound layer, the black circles in Fig. 4 show the values of diffusion coefficient D with varying NP mass (but fixed radius) (the translational D is obtained from the asymptotic behavior of $\mathrm{MSD}_{\mathrm{trans}}$, and the rotational diffusion is calculated by the relaxation time of the orientation autocorrelation function[30]).

We can describe the mass dependence of D (rotational and translational) with a simple power-law relation, $D = A_0/m^{\delta}$, where A_0 and δ are the fit parameters. Since we find $\delta \approx 1/3$ for systems with a fixed NP size but varying mass, we conjecture that the change in mass has the same effect as an effective change in the NP size. Because we are interested in the mass dependence of the diffusion and this dependence is similar for both rotational and translational diffusion coefficients, we refer to both D_{r} (rotational diffusion) and D_{t} (translational diffusion) as D. This observation is particularly surprising since we have maintained the bare size of the NP fixed during these calculations. We conclude that, in the limit where the NPs are comparable in mass to the solvent molecules, their diffusivity apparently follows the Stokes–Einstein relationship, but with the caveat that their effective size appears to be larger.

Having established the dependence of D in the absence of a bound layer, we now consider how D behaves when there is a bound layer that increases the effective NP size and mass. The blue diamond in Fig. 4 shows D for a NP of mass 13 with a strongly bound layer ($\varepsilon_{\mathrm{p-np}}$ = 2; T = 0.5). Clearly, D is much smaller than that expected for a NP of that mass with no bound layer. To compare to the case of a NP without a bound polymer, we need to estimate the effective size (mass) of the NP with the bound layer. For this purpose, we use the sum of the NP mass and the chains bound to the surface of the NP.

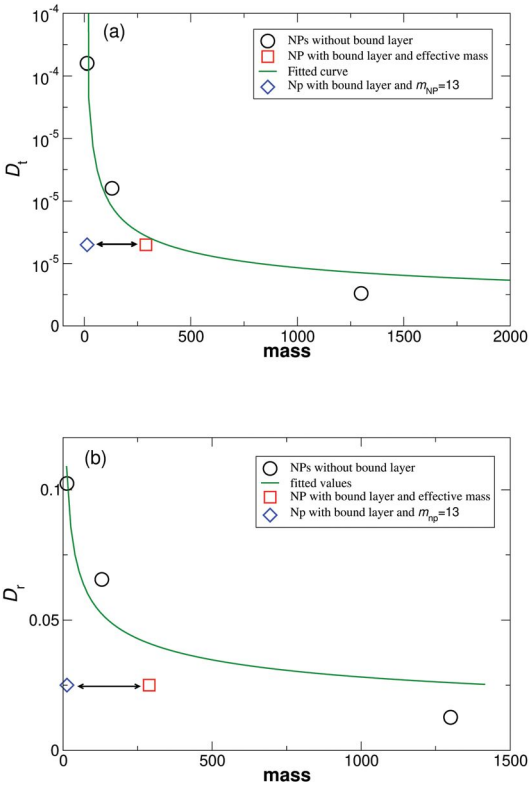

Fig. 4 (a) The NP translational diffusion coefficient for different values of mass and ε. Black circles are simulation data at T = 0.50 and ε = 1 where no bound layer forms. The green line is a fit of the black circles to A_0/m^{δ_t}, where A_0 = 0.0001, and δ_t = 0.35. The red square and the blue diamond are simulation data for ε = 2.0 and T = 0.50 with NP effective mass m = 289 (red square) and the bare NP mass m = 13 (blue diamond), respectively. (b) The NP rotational diffusion coefficient. The colors and symbols are the same as the translational diffusion coefficient descriptions. The qualitative behavior of the rotational and translation diffusion is similar. We fit the data to the B_0/m^{δ_r}. The fit parameters are B_0 = 0.23 and δ_r = 0.33. Interestingly, the translational and rotational diffusion coefficients follow similar power laws as a function of mass.

On average there are 13.8 chains in contact with the NP. Since each chain is composed of 20 monomers and the NP has 13 sites (each of unit mass), the effective NP mass is 13.8 × 20 + 13 = 289. The effective size then is increased by a factor of $289^{1/3}$. Interestingly, the use of this effective size (mass) for the NP with the bound layer results in close agreement with the diffusion coefficient of bare NPs of different masses but with no bound layer. These results suggest that the increase in the size of the NP due to the bound layer is the major cause of the slowdown in NP diffusion.

To emphasize the relevance of this result in experiments, we discuss a recent series of papers by Winey, Composto and co-workers.[31,32] In one case, they used 4.3 nm diameter iron oxide NPs grafted with PMMA chains and dispersed them in PMMA matrices with different molecular weights. They found that the NPs were slowed relative to the Stokes–Einstein prediction, and they used this slow-down to estimate the effective NP size. Depending on system specifics, they found an effective particle size of $2R_{eff}$ = 18–20 nm. To understand these results, we calculate the effective NP size, $R_c + h$, using a model,

$$\frac{4}{3}\pi(R_c + h)^3 \equiv \frac{4}{3}\pi {R_c}^3 + \frac{ZN}{\rho}, \quad (7)$$

that assumes the effective volume of a grafted NP is the (incompressible) sum of the volumes of the core (first term on the right side of the equation) and the polymeric corona (second term on the right); the idea of defining an effective particle with volume that is an incompressible sum of the NP and polymer segments has been verified by simulations.[33] Here R_c = 2.15 nm is the core radius, h is the effective brush height, $Z = 4\pi {R_c}^2\sigma$ is the number of grafted chains per NP, where each chain is of length N, σ is the grafting density (0.16–0.55 chains per nm^2 in a series of experiments) and ρ (≈1 g cm^{-3}) is the polymer density. For the particular choice of grafting parameters in the experiments we find $2R_{eff} \approx$ 16–21 nm, with the precise result depending on the grafting density. Since these results are in good agreement with experimental estimates, we conclude that the idea of the adsorbed layer increasing the effective NP size can describe diffusivity changes, at least in the case where the chains are chemically grafted to the NPs.

Going beyond these results, a parallel study by these researchers also measured the consequence of the physically adsorbed bound layers on NP diffusion in the case of poly(2-vinylpyridine)/silica nanocomposites.[32] They found a slowing down of NP diffusion, with this slowing down being more pronounced with increasing P2VP chain length. These results track our earlier work using TGA and indirectly TEM on the size of the bound polymer layer in these cases.[34,35] These results further support the validity of the explanation presented here and imply that the bound layer has measurable consequences on NP transport, well outside the self-intermediate scattering function.

4. Conclusion

We performed MD simulations of polymer nanocomposites to study the effects of NP motion on the apparent dynamics of the interfacial layer. Our results suggest that NP motion can suppress the longer-time relaxation signature of this bound layer in the scattering function. This is particularly true when the NPs are mobile on a time scale comparable to the polymers. However, since we find the NP diffusion to be mass-dependent, likely because the NP relaxation time is similar to that of the polymer chains, we propose an indirect method to measure the size (mass) of the bound layer. We show that the total volume of the NP and bound chains is a good estimate of the effective volume of the NP. The slowdown in the NP diffusion with the presence of the bound layer, in particular its dependence on the polymer chain molecular weight, is a direct consequence of the presence of a bound layer around NPs. Thus, while it is not easy to obtain clear signatures of this bound layer relaxation in the self-intermediate scattering function when NPs are relatively mobile, measurements of NP

diffusion might be an unequivocal means to critically characterize this physically adsorbed polymer layer, especially when it has a long temporal persistence.

Conflicts of interest

There are no conflicts to declare.

Acknowledgements

Computer time was provided by Columbia University. Financial support for this research was provided by the NSF through grant no. DMR-1709061 (SK, HE). This work was supported by NIST grant no. 70NANB19H137 (FS).

References

1 J. H. Koo, in *Optical Properties of Polymer Nanocomposites*, Cambridge University Press, 2016, pp. 550–565.
2 R. Gangopadhyay and A. De, *Chem. Mater.*, 2000, **12**, 608–622.
3 A. C. Balazs, T. Emrick and T. P. Russell, *Science*, 2006, **314**, 1107–1110.
4 G. Schmidt and M. M. Malwitz, *Curr. Opin. Colloid Interface Sci.*, 2003, **8**, 103–108.
5 J. F. Moll, P. Akcora, A. Rungta, S. Gong, R. H. Colby, B. C. Benicewicz and S. K. Kumar, *Macromolecules*, 2011, **44**, 7473–7477.
6 J. Jordan, K. I. Jacob, R. Tannenbaum, M. A. Sharaf and I. Jasiuk, *Mater. Sci. Eng., A*, 2005, **393**, 1–11.
7 S. K. Kumar, B. C. Benicewicz, R. A. Vaia and K. I. Winey, *Macromolecules*, 2017, **50**, 714–731.
8 J. Jancar, J. Douglas, F. W. Starr, S. Kumar, P. Cassagnau, A. Lesser, S. S. Sternstein and M. Buehler, *Polymer*, 2010, **51**, 3321–3343.
9 W. Caseri, *Macromol. Rapid Commun.*, 2000, **21**, 705–722.
10 E. Y. Lin, A. L. Frischknecht and R. A. Riggleman, *Macromolecules*, 2020, **53**, 2976–2982.
11 P.-C. Ma, N. A. Siddiqui, G. Marom and J.-K. Kim, *Composites, Part A*, 2010, **41**, 1345–1367.
12 T. Kashiwagi, F. Du, K. I. Winey, K. M. Groth, J. R. Shields, S. P. Bellayer, H. Kim and J. F. Douglas, *Polymer*, 2005, **46**, 471–481.
13 J. Fu and H. E. Naguib, *J. Cell. Plast.*, 2006, **42**, 325–342.
14 F. W. Starr, J. F. Douglas and S. C. Glotzer, *J. Chem. Phys.*, 2003, **119**, 1777–1788.
15 J. B. Hooper and K. S. Schweizer, *Macromolecules*, 2006, **39**, 5133–5142.
16 F. W. Starr, J. F. Douglas, D. Meng and S. K. Kumar, *ACS Nano*, 2016, **10**, 10960–10965.
17 P. Rittigstein, R. D. Priestley, L. J. Broadbelt and J. M. Torkelson, *Nat. Mater.*, 2007, **6**, 278–282.
18 A. P. Holt, P. J. Griffin, V. Bocharova, A. L. Agapov, A. E. Imel, M. D. Dadmun, J. R. Sangoro and A. P. Sokolov, *Macromolecules*, 2014, **47**, 1837–1843.
19 A. P. Holt, J. R. Sangoro, Y. Wang, A. L. Agapov and A. P. Sokolov, *Macromolecules*, 2013, **46**, 4168–4173.
20 S. E. Harton, S. K. Kumar, H. Yang, T. Koga, K. Hicks, E. Lee, J. Mijovic, M. Liu, R. S. Vallery and D. W. Gidley, *Macromolecules*, 2010, **43**, 3415–3421.
21 H. Emamy, S. K. Kumar and F. W. Starr, *Phys. Rev. Lett.*, 2018, **121**, 207801.
22 W. Zhang, H. Emamy, B. A. Pazmiño Betancourt, F. Vargas-Lara, F. W. Starr and J. F. Douglas, *J. Chem. Phys.*, 2019, **151**, 124705.
23 H. Emamy, S. K. Kumar and F. W. Starr, *Macromolecules*, 2020, **53**(18), 7845–7850.
24 A. Y. Liu, H. Emamy, J. F. Douglas and F. W. Starr, *Macromolecules*, 2021, **54**, 3041–3051.
25 F. W. Starr, T. B. Schroder and S. C. Glotzer, *Macromolecules*, 2002, **35**, 4481–4492.
26 G. S. Grest and K. Kremer, *Phys. Rev. A*, 1986, **33**, 3628–3631.
27 S. Plimpton, *J. Comput. Phys.*, 1995, **117**, 1–19.
28 T. Desai, P. Keblinski and S. K. Kumar, *J. Chem. Phys.*, 2005, **122**, 134910.
29 J. Liu, D. Cao and L. Zhang, *J. Phys. Chem. C*, 2008, **112**, 6653–6661.
30 D. Heyes, *J. Chem. Phys.*, 2019, **150**, 184503.
31 C.-C. Lin, P. J. Griffin, H. Chao, M. J. Hore, K. Ohno, N. Clarke, R. A. Riggleman, K. I. Winey and R. J. Composto, *J. Chem. Phys.*, 2017, **146**, 203332.
32 P. J. Griffin, V. Bocharova, L. R. Middleton, R. J. Composto, N. Clarke, K. S. Schweizer and K. I. Winey, *ACS Macro Lett.*, 2016, **5**, 1141–1145.
33 J. Midya, M. Rubinstein, S. K. Kumar and A. Nikoubashman, *ACS Nano*, 2020, **14**(11), 15505–15516.
34 N. Jouault, J. F. Moll, D. Meng, K. Windsor, S. Ramcharan, C. Kearney and S. K. Kumar, *ACS Macro Lett.*, 2013, **2**, 371–374.
35 N. Jouault, M. K. Crawford, C. Chi, R. J. Smalley, B. Wood, J. Jestin, Y. B. Melnichenko, L. He, W. E. Guise and S. K. Kumar, *ACS Macro Lett.*, 2016, **5**, 523–527.